JOURNAL OF GEOPHYSICAL RESEARCH, VOL. 113, E06004, doi:10.1029/2007JE002939, 2008

Martian dunite NWA 2737: Integrated spectroscopic analyses of brown olivine

Carle M. Pieters,[1] Rachel L. Klima,[1] Takahiro Hiroi,[1] M. Darby Dyar,[2] Melissa D. Lane,[3] Allan H. Treiman,[4] Sarah K. Noble,[5] Jessica M. Sunshine,[6] and Janice L. Bishop[7,8]

Received 5 October 2007; revised 13 December 2007; accepted 6 March 2008; published 18 June 2008.

[1] A second Martian meteorite has been identified that is composed primarily of heavily shocked dunite, Northwest Africa (NWA) 2737. This meteorite has several similarities to the Chassigny dunite cumulate, but the olivine is more Mg rich and, most notably, is very dark and visually brown. Carefully coordinated analyses of NWA 2737 whole-rock and olivine separates were undertaken using visible and near-infrared reflectance, midinfrared emission and reflectance, and Mössbauer spectroscopic studies of the same samples along with detailed petrography, chemistry, scanning electron microscopy, and transmission electron microscopy analyses. Midinfrared spectra of this sample indicate that the olivine is fully crystalline and that its molecular structure remains intact. The unusual color and spectral properties that extend from the visible through the near-infrared part of the spectrum are shown to be due to nanophase metallic iron particles dispersed throughout the olivine during a major shock event on Mars. Although a minor amount of Fe^{3+} is present, it cannot account for the well-documented unusual optical properties of Martian meteorite NWA 2737. Perhaps unique to the Martian environment, this "brown" olivine exhibits spectral properties that can potentially be used to remotely explore the pressure-temperature history of surface geology as well as assess surface composition.

Citation: Pieters, C. M., R. L. Klima, T. Hiroi, M. D. Dyar, M. D. Lane, A. H. Treiman, S. K. Noble, J. M. Sunshine, and J. L. Bishop (2008), Martian dunite NWA 2737: Integrated spectroscopic analyses of brown olivine, *J. Geophys. Res.*, *113*, E06004, doi:10.1029/2007JE002939.

1. Introduction

[2] More than 30 Martian meteorites provide direct and detailed information about the mineralogy, chemistry, and age of materials that form the crust of Mars. The shergottites are basaltic in nature, and nakhlites are augite cumulates from basaltic magmas [e.g., *Treiman et al.*, 2000; *McSween*, 2002]. Chassigny, until recently in a class by itself, is composed almost entirely of an olivine cumulate (dunite) from a basaltic magma. In 2005, a second chassignite, the meteorite Northwest Africa (NWA) 2737, was recognized [*Beck et al.*, 2005, 2006; *Mikouchi*, 2005; *Treiman et al.*, 2007]. Unlike the classic visually green olivine of Chassigny, however, the NWA 2737 dunite appears visually dark: almost black in hand sample and dark brown in thin section.

[3] Although the Martian meteorites provide detailed compositional information, their source areas on the planet are not known, and consequently there is no linked geologic context that can constrain the character and evolution of the Martian surface. Instead, we currently must rely on compositional information from orbital remote sensing and in situ experiments to provide boundaries to such global- and regional-scale issues.

[4] The unusual optical characteristics of NWA 2737 and the importance of olivine in crustal composition and evolution make it particularly relevant to identify the processes that have influenced this meteorite's properties. Addressing such issues requires integrated spectroscopic and petrologic investigations. We have carefully prepared samples of NWA 2737 to allow multiple analytical techniques to be applied to the exact same sample. A detailed petrographic investigation of our sample of NWA 2737 is presented in a companion paper [*Treiman et al.*, 2007]. We have obtained a series of coordinated laboratory spectra from this chip of NWA 2737 and derived particulate separates across the broad range of wavelengths where features diagnostic of specific minerals occur. The objective of our work is to present the diverse laboratory spectroscopic data for

[1]Department of Geological Sciences, Brown University, Providence, Rhode Island, USA.
[2]Department of Astronomy, Mount Holyoke College, South Hadley, Massachusetts, USA.
[3]Planetary Science Institute, Tucson, Arizona, USA.
[4]Lunar and Planetary Institute, Houston, Texas, USA.
[5]Astromaterials Research and Exploration Science Division, Johnson Space Center, Houston, Texas, USA.
[6]Department of Astronomy, University of Maryland, College Park, Maryland, USA.
[7]NASA Ames Research Center, Mountain View, California, USA.
[8]Search for Extraterrestrial Intelligence Institute, Mountain View, California, USA.

0148-0227/08/2007JE002939$09.00

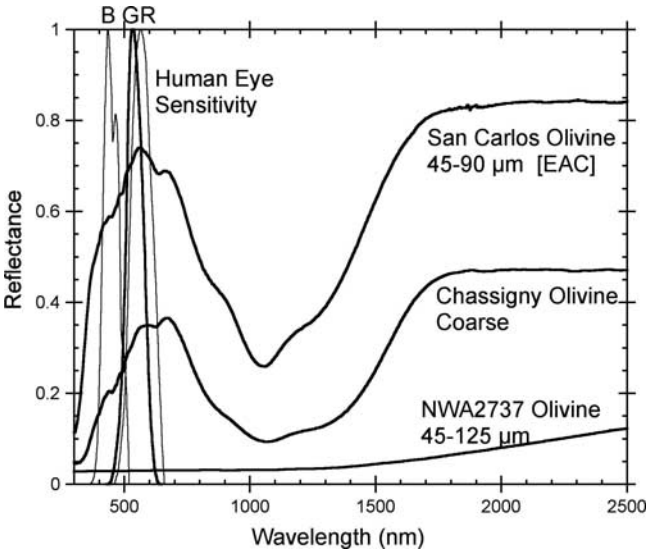

Figure 1. Visible and near-infrared spectra of coarse-grained San Carlos, Chassigny, and NWA 2737 olivines. Normal olivine appears green or yellowish to the human eye because of its peak reflectance near 550 nm. At near-infrared wavelengths, olivine is distinguished by its prominent composite crystal field absorption near 1000 nm caused by Fe^{2+} in octahedral M1 and M2 sites. NWA 2737 olivine exhibits a very low albedo in the visible and a continuous red slope toward longer wavelengths; the diagnostic features of olivine are not clearly evident in the spectrum.

NWA 2737 in the context of the sample's petrology and to discuss the implications of these data to remote sensing and in situ measurements of Mars.

2. Color of Olivine

[5] To the human eye, the mineral olivine normally appears green or yellowish green in hand sample and clear or yellowish in thin section. As illustrated in Figure 1, this color is due to a peak in visible reflectance that typically occurs near 550 nm. At the longer, near-infrared wavelengths measured by laboratory spectrometers, olivine is distinguished by a prominent composite absorption band composed of three superimposed crystal field absorptions near 1000 nm caused by electronic transitions of Fe^{2+} in the octahedral M1 and M2 sites [*Burns*, 1970; *Sunshine and Pieters*, 1998].

[6] The multicomponent crystal field absorption near 1000 nm is shown in Figure 1; it varies with particle size (which controls the average path length through grains). Strong bands are typical of large particles. Coarse-grained samples of two well-known olivine samples are shown: Chassigny olivine is Fo_{69}, and San Carlos olivine from Arizona is Fo_{91}. For comparison, a coarse-grained sample of NWA 2737 olivine (Fo_{78}) exhibits dramatically different optical properties even though its Mg/Fe composition is intermediate between these other two. Reflectance at all wavelengths is lower than for the two more typical olivines shown. Shorter wavelengths are suppressed to the greatest extent, hence the brown appearance to the human eye for NWA 2737.

[7] As will be discussed, largely in section 6, the visual color of olivine can be affected by several factors including the composition of the olivine (largely Mg/Fe) and the oxidation state of the iron (abundance of Fe^{3+}). However, the cause of the unusual properties observed for NWA 2737 comes from a completely unexpected source that we describe in this paper. We compare the properties of NWA 2737 with other Martian meteorites (Chassigny and ALH A77005) and several relevant terrestrial olivines.

3. Sample Preparation and Methods

3.1. NWA 2737

[8] Coordinated petrographic and spectroscopic characterization began with a 1.75 g fragment of NWA 2737 obtained from the finders, Bruno Fectay and Carine Bidaut of *La Memoire de la Terre*. The fragment was mounted and halved at the Lunar and Planetary Institute. One half of the fragment was prepared as a polished thin section for investigation of the petrography, mineral chemistry, and deformation/shock history of NWA 2737. These data and supportive Mössbauer spectra and micro-XANES spectra are discussed in detail by *Treiman et al.* [2007].

[9] The half of the NWA 2737 fragment without Crystalbond or epoxy (~0.5 g) was reserved for optical spectral measurements. This chip was first analyzed at Arizona State University (ASU) for measurement of a whole-rock thermal emission spectrum. The chip was then forwarded to Mount Holyoke, where it was again split in half. One of these portions was gently ground to make a whole-rock powder, which was sieved to <45 μm and >45 μm size fractions. The final portion of NWA 2737 was coarsely crushed and separated by handpicking into mineral fractions of olivine and pyroxene. Because this method uses color, grain morphology, and cleavages to distinguish among the different phases present, it is not a perfect science in situations such as this one where grains of coexisting species have similar appearances. The separates thus obtained were crushed and sieved in the same manner as the whole rock. All mineral separates and rock powders were sent to Brown University for measurement of visible, near-IR, and mid-IR reflectance. The separates and powders were then taken to ASU for acquisition of thermal emission spectra. Finally, the separates and powders were returned to Mount Holyoke for acquisition of Mössbauer spectra. Full Mössbauer spectra, methods, and deconvolutions for NWA 2737 are presented by *Treiman et al.* [2007]. A more detailed integrated analysis of Mössbauer spectra for Martian meteorites is given by *Dyar* [2003].

[10] Emissivity spectra (2000–250 cm^{-1}) were obtained at ASU using a modified Nicolet Fourier transform infrared (FTIR) spectrometer equipped with a CsI beam splitter and an uncooled DTGS detector. The system atmosphere is scrubbed using a Parker Balston compressed air and gas inline filter, and the sample chamber is kept at a constant temperature (~24.7°C). The samples were maintained at ~80°C using a sample cup heater, and the spectra were acquired over 270 scans at 2 cm^{-1} sampling. Details of the instrument calibration and data reduction strategy can be found in work by *Ruff et al.* [1997]. Sample size was

adequate for emission measurements of the meteorite chip and the two whole-rock powders; the amount of material available for the mineral separates was insufficient for emission measurement.

[11] Visible to near-infrared bidirectional reflectance spectra (0.3–2.6 μm, sampled at 5 nm increments) were acquired relative to halon at 30° incident, 0° emergent angles using the Reflectance Experiment Laboratory (RELAB) bidirectional spectrometer. The data were then corrected for the properties of halon. The same samples (in the same dish) were measured using a Pike diffuse reflectance attachment (off-axis, biconical) with the Thermo Nexus 870 FTIR spectrometer (2–50 μm, 5000–200 cm^{-1}) located at RELAB, using a diffuse gold standard. The FTIR spectra were obtained in a purged environment (H_20 and CO_2 free). The data were typically spliced to the near-infrared data at 2.5 μm to use the absolute reflectance of the bidirectional system. Detailed descriptions of the RELAB facility instruments can be found in the overview by *Pieters and Hiroi* [2004] (RELAB information is also available at http://www.planetary.brown.edu/relab/). All samples of the whole-rock powders and the olivine separates were adequate for both types of RELAB reflectance measurements.

3.2. ALH A77005

[12] Separates of Martian meteorite ALH A77005 were prepared by handpicking for coordinated spectroscopic analyses. Whole-rock and mineral separates were measured in the RELAB in the same manner as those of NWA 2737. Bidirectional reflectance spectra were measured (0.3–2.6 μm) and spliced to midinfrared reflectance spectra (2–50 μm) of the same samples.

3.3. Synthetic and Natural Olivines

[13] For comparison with the Martian olivines, optical spectra of a series of terrestrial mantle olivines were acquired. These samples are from peridotite nodules collected at Kilborne Hole, New Mexico and Dish Hill, California by Anne McGuire. The chemistries, Mössbauer spectra, and metasomatic history of these samples are discussed by *McGuire et al.* [1991], *Banfield et al.* [1992], and *Dyar et al.* [1992]. For the Kilborne Hole sample, metasomatism has not resulted in oxidation of iron in the olivines [*Dyar et al.*, 1992]. However, the samples from Dish Hill do show a change in oxidation state of iron related to the metasomatism [*McGuire et al.*, 1991; *Banfield et al.*, 1992]. These olivine compositions are $\sim Fo_{87-92}$.

[14] Also used for comparison here are the optical and Mössbauer spectra of two synthetic high-iron olivines with compositions of $\sim Fo_{30}$. One of the samples was synthesized in the Department of Earth Sciences, Bristol University, United Kingdom using procedures described by *Redfern et al.* [2000], as reported by *Menzies et al.* [2001]. The other was synthesized by Don Lindsley at State University of New York, Stony Brook as follows. A mixture of hematite and oxides was ground for 1–2 h under ethanol. An iron sponge was then added, and grinding continued for less than 1 h. The product was wrapped in silver foil and placed in a silicon glass capsule. One end was sealed, and the middle of the capsule was drawn out into a capillary, leaving the sample by the sealed end. An Fe getter was placed next to the open end of the capsule. The capsule was put into a vertical tube furnace at ~800°C (the Fe getter remained at ~600°C) for 10–20 min. The capsule was taken out of the furnace and sealed across the capillary. The completely sealed capsule section containing the sample was then placed in a horizontal tube furnace at ~920–940°C and cooked for 10 d. The composition and crystallinity of both synthetic olivines was verified by X-ray diffraction.

[15] Visible and near-infrared spectra were collected for the synthetic and natural mantle olivine samples using the same procedures outlined in section 3.1 for NWA 2737. Mössbauer analyses of these samples use the same methods as those described by *Treiman et al.* [2007]. Approximately 10–20 mg of each sample were mixed with sugar to allow distribution of a thin layer of sample across the holder. The sample-sugar mixture was gently ground under acetone to prevent oxidation and allow sugar to count the minerals' grains to mitigate effects of preferred orientation. The mixture was then mounted in a sample holder confined by Kapton tape (see *Dyar* [2003] for experimental techniques). Mössbauer spectra were acquired at room temperature using a source of 30 mCi ^{57}Co in Rh on a WEB Research Co. model W100 spectrometer. Run times were 8–12 h, and results were calibrated against α-Fe foil. Spectra were processed using the DIST_3D program, an implementation of software described by *Wivel and Mørup* [1981]. The program uses quadrupole-splitting distributions with Lorentzian lineshapes and an assumed average correlation between the isomer shift (IS) and quadrupole shift (QS) in each of two valence states. Widths, isomer shifts, and quadrupole splittings of the doublets were allowed to vary. Errors on IS and QS for well-resolved peaks are usually ±0.02 mm s^{-1}. Errors on peak area depend on the extent of overlap with other peaks but are generally ±3–5% absolute. See *Treiman et al.* [2007] for Mössbauer fitting results of NWA 2737.

4. Characteristics of NWA 2737

[16] The chemistry of the NWA 2737 meteorite has been described by *Connolly et al.* [2006] and *Beck et al.* [2006]. The petrology and shock history of the specific sample analyzed with spectroscopic techniques here are described in detail along with chemical data in the paper by *Treiman et al.* [2007].

[17] *Treiman et al.* [2007] report that this sample of NWA 2737 is a dunite consisting of ~87% olivine, ~6% pyroxene (augite, pigeonite, and orthopyroxene), ~3% chromite, and ~4% other phases including feldspathic and granitic glass, kaersutite amphibole, ilmenite, apatite, rutile, and FeS. The olivine has an Mg# of 78, and micro-XANES and Mössbauer spectroscopy indicate that it contains a measurable but small amount of Fe^{3+}. Chromite is found as separate grains or as inclusions within the olivine. The Fe^{3+} detected by Mössbauer spectroscopy for NWA 2737 olivine is less than 3% of total iron but greater than zero. In thin section, the olivine is predominately visually brown colored, although thin bands of visually colorless olivine appear dispersed throughout. The bands of visually colorless olivine are not random and appear to be oriented with long axes along $\underline{a}$([100]) and short and intermediate axes near {021} planes.

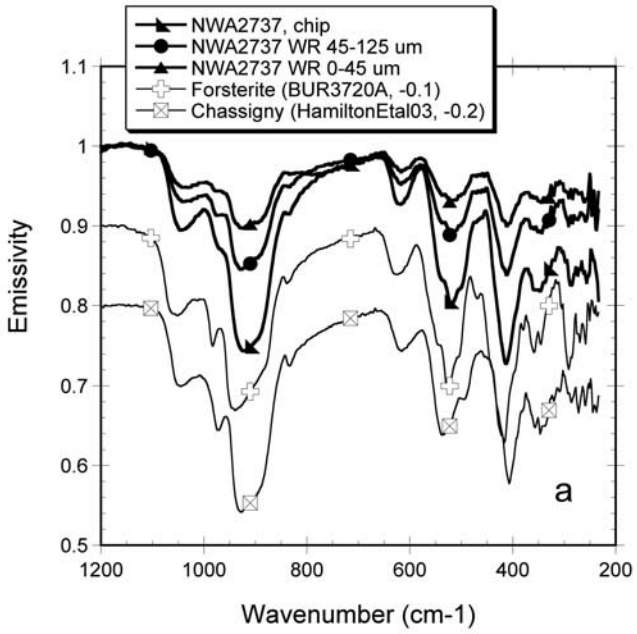

Figure 2a. Emissivity spectra of NWA 2737 compared with emission spectra of a library forsterite (BUR3720A) and of the Chassigny meteorite.

[18] Nanophase iron particles with diffraction patterns consistent with α-iron (kamacite) are found dispersed throughout the visually brown olivine [*Reynard et al.*, 2006; *Beck et al.*, 2006; *Treiman et al.*, 2007]. No nanophase magnetite was detected by either transmission electron microscopy (TEM) or Mössbauer in our sample of NWA 2737. This was important to note because nanophase magnetite could have had a significant optical effect.

[19] NWA 2737 has clearly undergone one or more significant shock events. Pervasive shock features are observed, including planar deformation features, micron-scale discontinuous lamella, mosaicized texture, and lattice distortions at the atomic scale [*Beck et al.*, 2006; *Reynard et al.*, 2006; *Treiman et al.*, 2007]. The visually clear bands of olivine are observed within the brown olivine and are more heavily cracked than the dominant brown olivine. The brown olivine appears a little brighter in backscattered electron (BSE) imagery [*Treiman et al.*, 2007], implying a slightly greater electron density. The brighter appearance of the brown olivine compared to the compositionally equivalent clear olivine in BSE imagery suggests an overall more dense structure, consistent with the Raman spectra from work by *Reynard et al.* [2006] and *Beck et al.* [2006]. Although the crystallization age of this Martian meteorite appears to be 1.42 Ga [*Misawa et al.*, 2005], *Bogard and Garrison* [2006] identify a major event that completely degassed the sample of radiogenic ^{40}Ar between 160 and 170 Ma ago.

4.1. Emissivity: Midinfrared (8.3–50 μm or 1200–200 cm^{-1})

[20] Emissivity spectra of NWA 2737 whole-rock samples (chip, 45–125 μm, and <45 μm fractions) are shown in Figure 2a. As is typical for silicates, the fundamental vibrational features become less pronounced with decreasing particle size (i.e., shallower, higher emissivity), and volume scattering features become more pronounced. The SiO_4 groups in olivine are distorted Td groups with Cs symmetry and have been well characterized with transmittance spectra; absorptions due to SiO_4 include a symmetric ν_1 vibration near 830 cm^{-1}, symmetric ν_2 vibration near 370 cm^{-1}, asymmetric ν_3 vibration triplet between 825 and 1000 cm^{-1}, and an asymmetric ν_4 vibration triplet between 460 and 610 cm^{-1} in transmittance spectra [*Duke and Stephens*, 1964; *Tarte*, 1963]. The band positions and shape are shifted slightly for reflectance and emittance spectra compared to transmission spectra because both the real and imaginary optical constants contribute to the former. Volume scattering behavior in the <45 μm fraction often produces a feature between ~840 and 650 cm^{-1} that deepens with decreasing particle size [e.g., *Aronson et al.*, 1966; *Hunt and Vincent*, 1968; *Conel*, 1969; *Salisbury and Eastes*, 1985; *Mustard and Hays*, 1997; *Lane*, 1999; *Cooper et al.*, 2002].

[21] Comparison of the NWA 2737 meteorite spectra to a library spectrum of forsteritic olivine (Mg-rich BUR3720A [*Christensen et al.*, 2000]) in Figure 2a confirms the general forsteritic chemistry of NWA 2737 olivine. No bands of the whole-rock NWA 2737 emissivity spectra can be directly attributable to minerals other than olivine, although formal deconvolution with library spectra could be consistent with a few percent of augite pyroxene. Because the library olivine is more magnesian (Fo_{92}) than that of NWA 2737 (Fo_{78}), the spectral bands of the library olivine are at slightly higher frequencies (larger wave numbers) than the bands in NWA 2737 spectra in Figure 2a (e.g., see trends in works by *Burns and Huggins* [1972], *Jeanloz* [1980], and *Hofmeister* [1997]).

[22] The single mismatch between the library olivine spectrum and those of NWA 2737 is that the rock chip spectrum does not show the distinct band at ~980 cm^{-1}

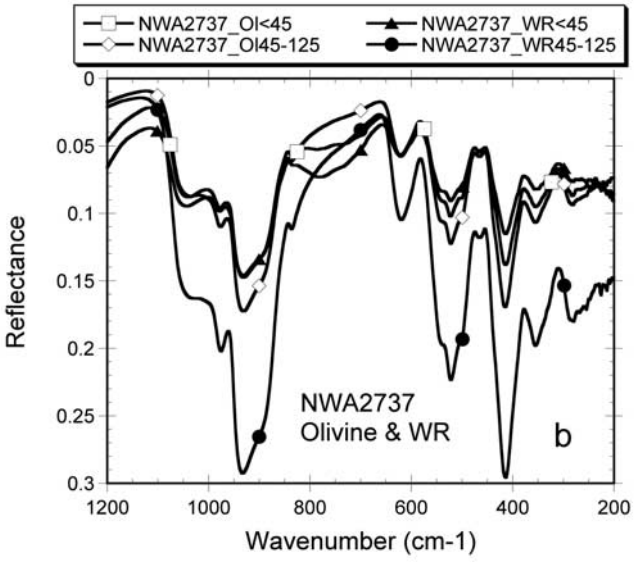

Figure 2b. Midinfrared reflectance spectra (inverted for comparison with emissivity) of the NWA 2737 whole-rock and olivine separates.

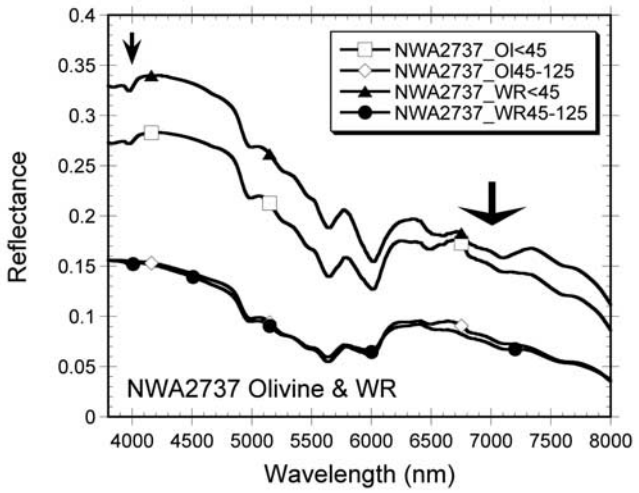

Figure 3. Mid-IR reflectance spectra of the NWA 2737 whole-rock and olivine separates. Arrows indicate carbonate absorptions; all other features are due to olivine.

(Figure 2a). Although this difference remains unresolved, a possible explanation is that the olivine in the measured rock chip had a preferred orientation. The ~980 cm^{-1} feature arises from emission whose electronic vector is parallel to the *y* axis of olivine [*Fabian et al.*, 2001], and so its absence in the rock chip spectrum could suggest a reduced contribution of that energy reaching the detector as a result of crystal orientation. In thin section [*Treiman et al.*, 2007], we did not note a preferred orientation of olivine grains, but a few other Martian meteorites do show preferred orientations of their mineral grains [e.g., *Berkley and Keil*, 1981]. The thermal emissivity spectrum of the NWA 2737 chip is similar to that of Chassigny [*Hamilton et al.*, 2003], except that the spectral bands are at a higher frequency because of higher magnesium of the NWA olivine.

4.2. Reflectance: Midinfrared (3.8–50 μm or 2650–200 cm^{-1})

[23] Infrared reflectance (*R*) spectra can be related to emission (*E*) spectra by Kirchhoff's law ($E = 1 - R$). Shown in Figure 2b are reflectance spectra of the NWA 2737 samples, both whole-rock as well as olivine separates. The scales of the graphs are inverted for comparison with the emission spectra of Figure 2a. The shape and character of absorption features in the reflectance spectra are directly comparable to those of the thermal emission spectra, whereas the difference in absolute magnitude of features is largely a geometry effect. The reflectance spectra of the olivine separates (<45 μm and 45–125 μm) shown here are comparable to the reflectance and emission spectra of the whole-rock samples, indicating that the olivine separates dominate the spectral character of the sample in this wavelength region. The only significant difference between the reflectance and emission spectra of Figure 2 is the transparency feature between 800 and 650 cm^{-1}, which is more prominent in fine-grained reflectance spectra than in the emission spectra. The transparency feature does not affect spectral analyses, however, because no diagnostic fundamental vibrational bands occur at these frequencies. These reflectance spectra of the particulate samples also exhibit a more pronounced ~980 cm^{-1} component of the ν_3 triplet than observed in the emissivity spectra.

[24] Prominent combination and overtone vibrational features of olivine [e.g., see *Salisbury*, 1993] also occur in reflectance spectra of both the whole-rock and olivine separates at shorter wavelengths between 4000 and 8000 nm. These are illustrated in Figure 3 (note that below 8000 nm or above 1250 wave number, spectra will be shown as functions of wavelength rather than wave number). In addition to the olivine bands between 5500 and 6000 nm, distinct but weak features due to carbonate (indicated by arrows) are observed near 4000 and 7000 nm in both fine-grained samples, although the longer-wavelength emissivity and reflectance spectra did not exhibit any features resulting from carbonate. This identification is consistent with the trace amounts of carbonate identified in the sample [*Treiman et al.*, 2007].

[25] Molecular vibrational features observed in these midinfrared reflectance (and emissivity) spectra are dominated by olivine, confirming that NWA 2737 is indeed a well-crystallized dunite. The positions of all the spectral features observed are those predicted for the composition of the olivine (Fo_{78}) [*Lane and Dyar*, 2007]. With the exception of a small amount of carbonate, no bands between 3.8 and 50 μm for the whole-rock bulk sample or the olivine separates are indicative of the presence of significant amounts of any mineral other than olivine. Furthermore, at these wavelengths, there is no indication that the olivine is anything other than normal crystalline forsteritic olivine.

4.3. Reflectance: Visible to Near-IR (0.3–2.6 μm)

[26] Visible to near-infrared spectra of the whole-rock and olivine mineral separates of NWA 2737 are presented in Figure 4. In stark contrast to the midinfrared spectra of the

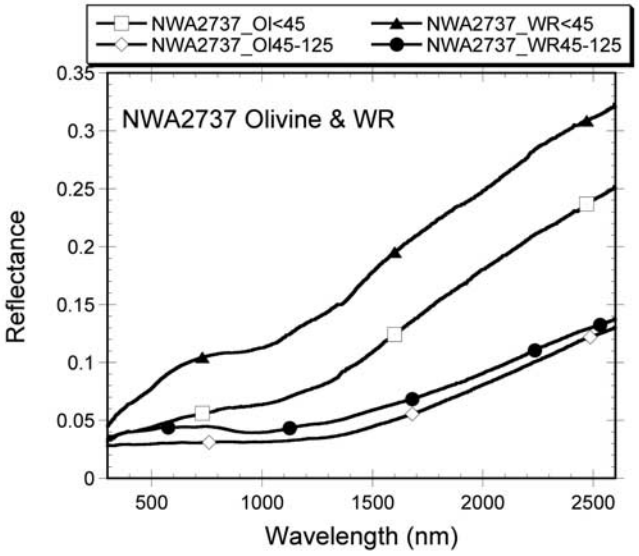

Figure 4. Visible near-IR reflectance spectra for the NWA 2737 whole-rock and olivine separates. All spectra display a very steep red-sloped continuum. The composite crystal field band at 1000 nm is barely visible because of the strong slope and low total reflectance.

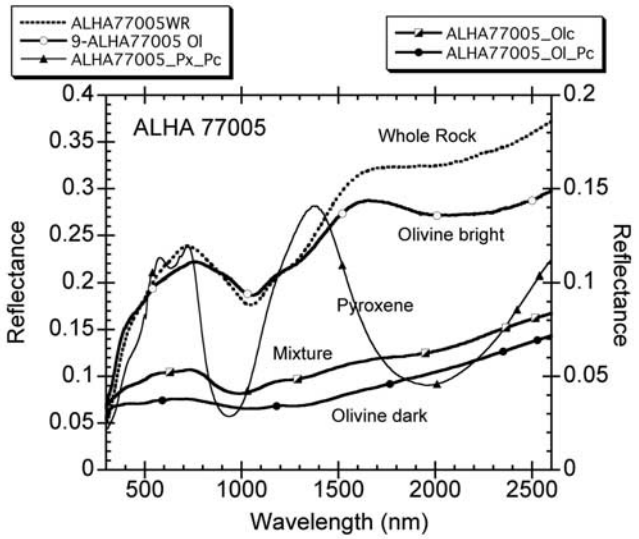

Figure 5. Visible to near-infrared reflectance spectra of whole-rock and mineral separates from ALH A77005. Note the scale for (right) the two darker separates is half that for (left) the brighter samples.

very same samples, these spectra are not immediately recognizable as olivine. In particular, the diagnostic crystal field absorptions, described in section 2 and shown in Figure 1, are virtually indiscernible, particularly in the coarse-grained size fractions. The spectra as a whole are significantly darker than "normal" olivine of similar iron content and roughly 1 order of magnitude lower reflectance than those in Figure 1. In contrast to other olivine spectra, the NWA 2737 spectra of Figure 4 are dominated by a strong red slope, which increases sharply around 1400 nm. A hint of a 1000 nm absorption feature is present in the smallest <45 μm fractions.

[27] The visible and near-infrared characteristics of NWA 2737 are surprising and quite different than those observed in Chassigny or even in terrestrial olivine of diverse compositions [e.g., *Sunshine and Pieters*, 1998]. Without additional information, the spectra of Figure 4 would not be readily interpreted to be derived from an olivine sample. Nevertheless, the midinfrared spectra provide irrefutable evidence that these samples are indeed composed of crystalline forsteritic olivine, and there is no possibility of misidentification. What in this particular olivine is physically responsible for these unusual VNIR optical properties, and what happened to the olivine to produce them? To address these questions, we examine the range of color variations that occur in olivine as a function of both chemistry and environment.

5. Related Martian Meteorites: ALH A77005

[28] Dark olivine, perhaps visually similar to that in NWA 2737, has been observed in other Martian meteorites. *Ostertag et al.* [1984] described a brownish color of a cumulus olivine that occurs in the highly shocked shergottite ALH A77005. They originally suggested that the brown color of these ALH A77005 olivine grains could be due to Fe^{3+} at percent levels arising from a process associated with the shock event. The brown color of the olivine was attributed to a transformation that occurs during shock that appeared to be supported by shock experiments that produced similar results, only when performed in an oxidizing environment [*Bauer*, 1979]. Subsequent measurements by *Burns* [1989], however, indicated that Fe^{3+} present in the olivine of ALH A77005 occurs at much less than 1%. The association of the brown color of ALH A77005 olivine with extensive shock is nevertheless well documented [*Ostertag et al.*, 1984].

[29] ALH A77005 has also been studied by our consortium in order to help explain the interesting spectral character of NWA 2737. We have prepared several separates of ALH A77005 to concentrate different mineral species in order to evaluate their potentially diagnostic spectral properties over the visible to midinfrared wavelengths. The dominant mafic mineral of this meteorite is olivine, although some pyroxene is also present [*McSween et al.*, 1979; *Ikeda*, 1994]. It was difficult to cleanly separate individual species of this heavily shocked meteorite because the visual appearance of some pyroxene grains and the shocked olivine is similar. Our initial procedure produced a good pyroxene separate, but the original olivine separates appeared to be of mixed composition. A second more refined mineral separation procedure produced several separates of distinct optical properties that are useful for this discussion. Shown in Figure 5 are spectra for the whole rock, a pyroxene separate, a bright olivine separate (that contains chrome spinel inclusions), and two of the darkest mineral separates, one that is a mixture of pyroxene and olivine and one that is of relatively pure but dark olivine. Midinfrared reflectance spectra (not shown) of the pyroxene and two olivine separates verify their bulk mineralogy.

[30] Near-infrared spectra of ALH A77005 have also been presented in the survey of *McFadden and Cline* [2005]. Their whole-rock powder of this meteorite clearly contains more pyroxene than the sample we received, but their spectra of different areas on a separate meteorite chip are fully consistent with the diversity of spectra shown in Figure 5. It should be noted that our whole-rock and higher albedo separates of this meteorite have more normal spectral characteristics of pyroxene and olivine as well as shergottites in general. The concentrated dark olivine separate of ALH A77005 exhibits near-infrared properties quite comparable to those of NWA 2737, namely, a very low albedo, weak ferrous crystal field absorptions, and a continuum that increases toward longer wavelengths. Influence of the notable red-sloped continuum of the dark olivine component can be seen in the ALH A77005 whole-rock spectrum. An important distinction of ALH A77005, however, is that not all the olivine is dark brown, and many grains remain quite optically normal. In addition, the pyroxenes of both ALH A77005 and NWA 2737 are not affected by whatever process produced the brown olivine (consistent with the shock loading experiments of *Bauer* [1979]).

[31] Comparing the near-infrared optical properties of mineral separates from Chassigny (Figure 1), NWA 2737 (Figure 4), and ALH A77005 (Figure 5) illustrates several points:

[32] 1. Although all these meteorite samples have been shocked, the visible and near-infrared properties of olivine constituents can vary considerably from sample to sample.

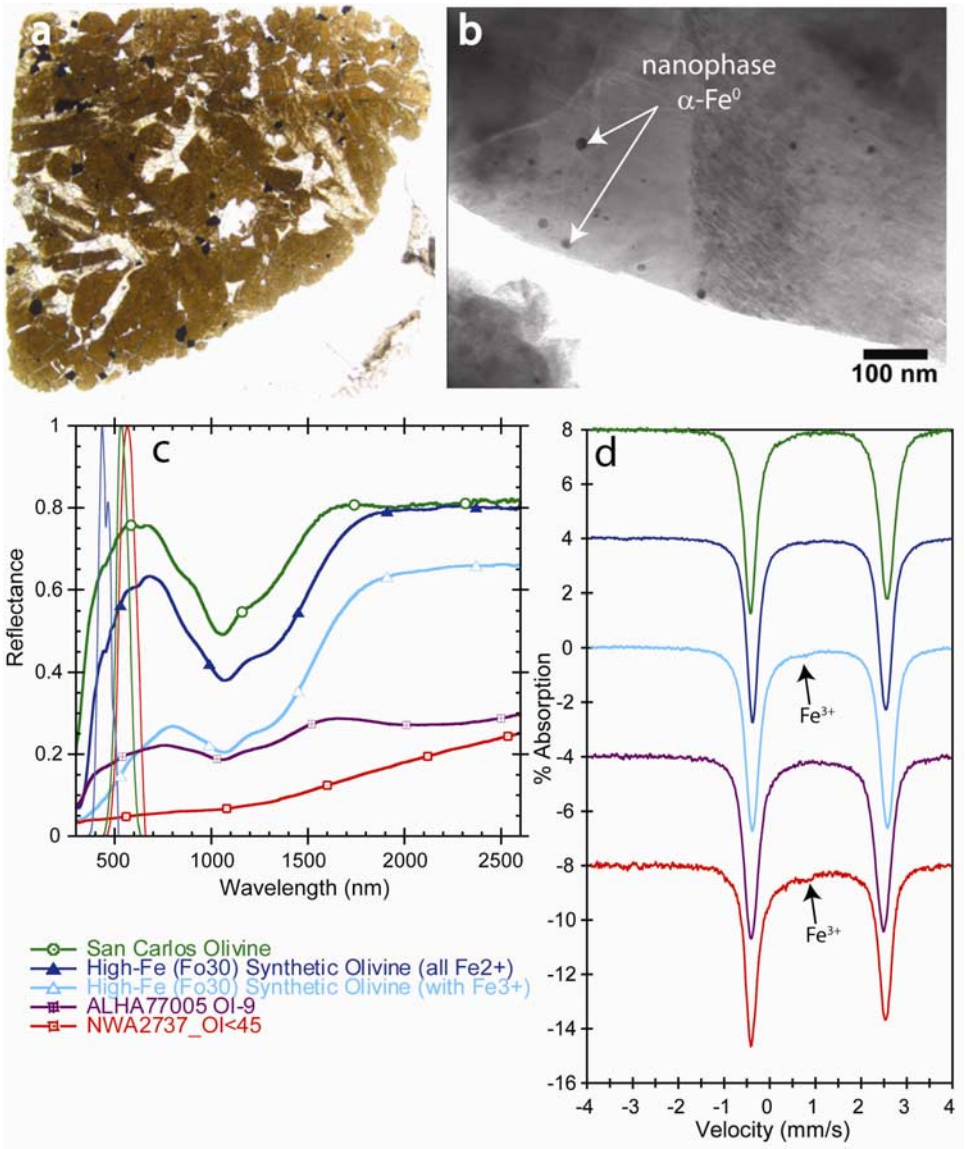

Figure 6. Overview of NWA 2737 properties. (a) Thin section of NWA 2737 illustrating brown color and texture of olivine. (b) Transmission electron microscope image of NWA 2737 olivine. Small, dark (electron-dense) spherules are consistent with α-iron kamacite [after *Treiman et al.*, 2007]. (c) Near-infrared spectra of olivine: San Carlos [normal] terrestrial olivine (Fo_{88}), synthetic high-iron (Fo_{30}) olivine (with only Fe^{2+}), synthetic high-iron (Fo_{30}) olivine (with Fe^{3+}), and olivine separates from SNC meteorite ALH A77005 and NWA 2737. (d) Mössbauer spectra of same olivines. Spectra are scaled and offset for comparison with one another.

[33] 2. Characteristics of the near-infrared spectra for the dark (brown) olivine are consistent when the olivine is found in different Martian meteorites.

[34] 3. The optical properties of other mafic minerals such as pyroxene are unaffected by whatever process produced the brown olivine. Furthermore, midinfrared spectra of the exact same samples indicate that the crystalline nature of the brown olivine has not been affected.

6. Color of NWA 2737 Olivine

[35] The overall characteristics of NWA 2737 olivine are illustrated in Figure 6. On the macroscale, the generally brown visual color is shown in the transmitted light thin section image (Figure 6a). On a submicroscopic scale, finely dispersed nanophase iron particles are seen (Figure 6b). The visible and near-infrared spectral properties are unusual compared to those of similar and different compositions of typical olivine (Figure 6c). Some, but very little, of the iron occurs in the trivalent form, and none is detected in magnetic phases (Figure 6d). The character and implications of these general properties are discussed below.

6.1. Total Fe^{2+} Content

[36] At visible wavelengths, the color of olivine is affected by the iron content. When iron is in the divalent form, iron-rich fayalite is darker and more orange/brown than the more magnesium-rich forsterite [*King and Ridley*, 1987;

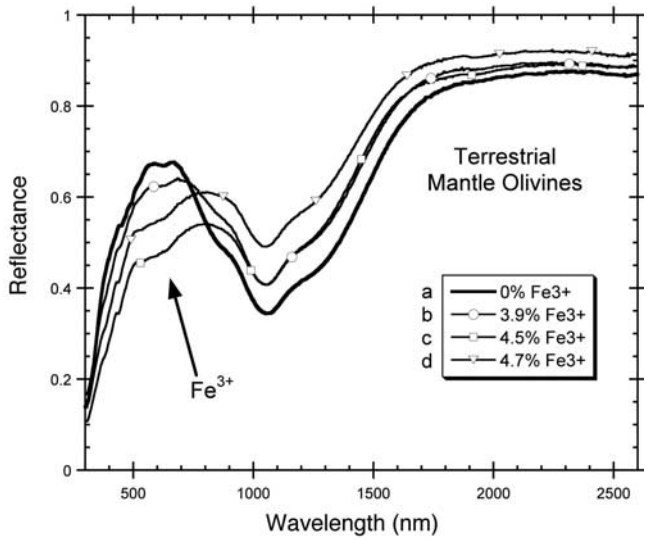

Figure 7. Terrestrial metasomatized forsteritic mantle olivines. (a) Kilborne Hole olivine has not experienced any Fe oxidation (0% Fe^{3+}). The Dish Hill samples ((b) 3.9% Fe^{3+}, (c) 4.5% Fe^{3}+, and (d) 4.7% Fe^{3+}), however, have experienced varying degrees of Fe oxidation during metasomatism. The %Fe^{3+} is reported as the percentage of total Fe atoms in the trivalent state. A Fe^{2+}-Fe^{3+} charge transfer near 650 nm (arrow) lowers their reflectance in the visible, and the olivines have a brownish appearance to the eye. Even at the higher-Fe^{3+} contents, the crystal field absorption near 1000 nm remains intact and prominent.

Sunshine and Pieters, 1998]. This is illustrated by comparing the forsterite (San Carlos) with the fayalite (synthetic Fo_{30} all Fe^{2+}), the top two spectra of Figure 6c. Although the human eye will detect a noticeable difference in color between these two, the crystal field bands near 1000 nm are well defined and remain highly diagnostic [*Sunshine and Pieters*, 1998].

[37] No amount of ferrous iron in the olivine can account for the strong spectral slope observed in NWA 2737, nor for the loss/weakening of crystal field absorption bands near 1000 nm. Furthermore, bulk chemical composition as a whole is not a factor in the strong visual coloring of NWA 2737 olivine, because the visually colorless and visually brown olivines both have the same chemical composition.

6.2. Fe^{3+} Content

[38] Replacement of Fe^{2+} with Fe^{3+} was originally believed to be the cause of the brown coloration of the unusual olivine observed in ALH A77005 [*Ostertag et al.*, 1984]. Spectra of terrestrial mantle olivines ($\sim Fo_{89}$) with various amounts of Fe^{3+} (reported as the percentage of total Fe atoms in the trivalent state) in the olivine structure are shown in Figure 7. Addition of Fe^{3+} to olivine enables a charge transfer between Fe^{2+} and Fe^{3+}, creating an absorption band near 625 nm. This in turn alters the visible color of olivine to a reddish brown. These Fe^{3+}-bearing mantle olivines are often referred to as visually brown. Although 3–5% Fe^{3+} causes the olivine to appear brown to the eye, the diagnostic crystal field olivine absorptions near 1000 nm remain intact and prominent.

[39] On the other hand, this visible effect can be profound in Fe^{3+}-bearing fayalitic olivines. The Fe^{2+}-Fe^{3+} charge transfer is enhanced strongly and affects a broad part of visible wavelengths. This is illustrated with the synthetic fayalite (Fa_{70}) that contains Fe^{3+} (middle blue spectra in Figure 6c). Furthermore, in the pure Fe^{3+} Fe^{2+} olivine, laihunite (RELAB collection, not shown), reflectance between 300 and 1400 nm is <4%. Between 1500 and 2000 nm, the reflectance of laihunite and similar Fe^{3+} olivines rises steeply, but the spectrum remains flat across the wavelength range 2000 and 2600 nm.

[40] The spectra of NWA 2737 (and those of some of the olivines in ALH A77005) are all dark in the visible range. The spectra of these Martian brown olivines, however, exhibit a red-sloping continuum that does not plateau but instead increases throughout the near infrared. In addition, significantly less than 3% of the iron present in NWA 2737 can be Fe^{3+} as constrained by Mössbauer, micro-XANES, and electromagnetic pulse chemical analyses (see discussion in the paper by *Treiman et al.* [2007]). Thus Fe^{3+} content of the NWA 2737 olivine by itself cannot be the origin of the brown color and anomalous visible and near-infrared properties of NWA 2737.

6.3. Nanophase Metallic Iron Particles ($npFe^0$)

[41] Small iron-rich nanophase particles have been observed throughout the NWA 2737 brown olivine. *Reynard et al.* [2006] describe them as less than 20 nm in size and composed of Fe-Ni metal alloy. These particles are only observed in the brown olivine; they are not seen in the clear olivine. *Reynard et al.* [2006] estimate the concentration of these particles in the olivine to be less than 0.1% of the total volume. TEM investigations of our sample described by *Treiman et al.* [2007] also observed the dispersed nanophase particles and identified them as α-iron (kamacite).

[42] It has been demonstrated experimentally that even tiny amounts of nanophase metallic iron particles in a silicate matrix (<0.05%) will have profound effects on the visible and near-infrared spectral properties of the host [*Noble et al.*, 2007]. The overall optical density (brightness) and spectral shape and slope of the resulting continuum are dependent on both the size and abundance of the embedded particles. These effects are illustrated in Figure 8 where increasing abundance of $npFe^0$ both darkens the spectrum and causes an overall red slope to the continuum that becomes more linear with increasing $npFe^0$, up to 0.3 wt% [after *Noble et al.*, 2007]. Although these experimental studies of $npFe^0$ were carried out to provide the basis for understanding space weathering on airless bodies [e.g., *Pieters et al.*, 2000; *Hapke*, 2001], they are directly applicable to understanding the unusual properties of NWA 2737 olivine. The abundance and small size of the nanophase particles observed for NWA 2737 predict that the visible albedo of the host should be low and the continuum should exhibit a pronounced slope toward longer wavelengths. Studies of space weathering also suggest that the presence of nanophase iron results in a severe reduction in the strength of characteristic mineral absorption bands. The size of the particles is important. Larger opaque or metallic particles in the 1–2 μm range simply darken a silicate host without imparting a red slope [*Britt and Pieters*, 1994], which also appears to be true of iron particles >$\sim$50 nm

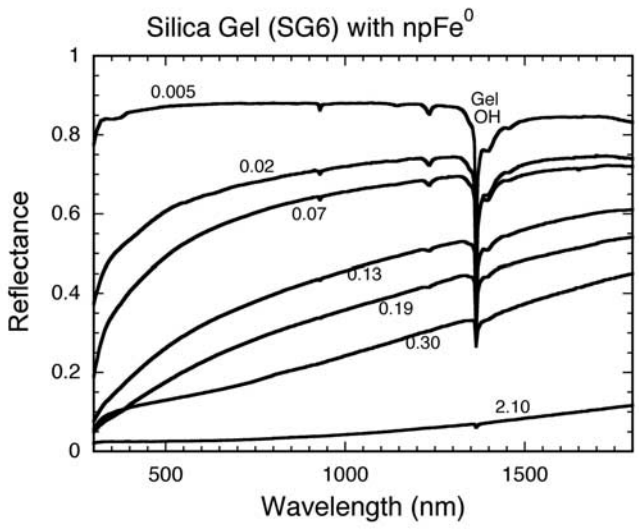

Figure 8. Reflectance spectra of silica gels impregnated with small amounts of nanophase metallic iron ($npFe^0$) [after *Noble et al.*, 2007]. The numbers indicate the wt% Fe in each sample. The OH feature at 1400 nm is in the silica gel.

[*Noble et al.*, 2007], which are small but significantly larger than those observed in NWA 2737. The striking similarity of the documented spectral effects of the small $npFe^0$ particles, coupled with their presence in the visually brown olivine and absence in visually clear olivine in NWA 2737, strongly suggest that $npFe^0$ may be the principal cause of the visible and near-infrared properties that dominate NWA 2737 spectra.

7. Discussion

[43] The origin of the brown olivine in NWA 2737 and the history of this meteorite are clearly intertwined. *Treiman et al.* [2007] proposed a two-shock event sequence to explain the relationship between the dominant brown olivine and the coexisting minor, but compositionally equivalent, clear olivine. In that scenario, a major impact event at ~170 Ma produced the pervasive brown olivine with shock features suggesting level S6 when the meteorite suffered ^{40}Ar loss [*Bogard and Garrison*, 2006]. The zones of clear olivine are attributed to postshock deformation and recrystallization of the brown olivine. A second smaller event, perhaps the one that launched the meteorite, was hypothesized to produce the shock features observed in the clear olivine.

[44] We propose a variant on this sequence that only requires the single major event at ~170 Ma to produce both the brown and the clear olivine of NWA 2737. We suggest the effective shock pressure and/or maximum temperature experienced by the small zones of clear olivine is slightly less than that experienced by the brown olivine host, but both are produced by the same event. The original olivine cumulate was transformed to brown olivine with its pervasive $npFe^0$ during this major impact event. We prefer this scenario because the presence of $npFe^0$ is currently the only viable component that accounts for the observed optical properties and the physical conditions required for its production and also because the formation requirements of the annealed and nonannealed zones [*Bauer*, 1979] appear to be met by a strong impact event in the Martian environment.

[45] The experimental shock-loading studies of olivine [*Bauer*, 1979] document that at high shock pressures (55–75 GPa). the intense short thermal pulse produces subsolidus annealing along with oxidation/reduction of Fe^{2+}, creating brown olivine when conditions include high pO_2 (10^{-4} atm (1 atm = $10^5 \times 1.01325$ N m^{-2})). Under lower-pO_2 (10^{-9} atm) conditions, annealing without the oxidation and coloration is observed. At pressures lower than ~64 GPa, experiments can contain mixed results (presumably resulting from a range of local shock pressures experienced), and some olivine grains exhibit both brown-colored annealed rims as well as colorless cores that retain high fracture densities and mosaic extinction patterns.

[46] As pointed out by *Treiman et al.* [2007], the orientation of clear olivine within the brown olivine host of NWA 2737 provides an important clue to its origin. In particular, the occurrence of clear olivine coincides with an easier slip orientation in olivine along {021} planes in the [100] direction at high temperatures (~1000°C) and low strain rates [*Cordier*, 2002; *Dunrick et al.*, 2005]. We suggest such a slip differential allows a minor amount of dissipation of shock pressures during the major shock event. The severity of the shock event was sufficient to instigate the redox process and transform almost all of the olivine present to annealed and $npFe^0$-bearing brown olivine, but it is hypothesized that minor slip along preferred orientations was sufficient to prevent the complete annealing of the grain, resulting in the observed zones and orientations of the heavily fractured but clear olivine. An interesting aspect of the deformation, however, is the relative inconspicuousness of deformation on the easiest high-temperature slip system for olivine, [100]{010}, and the prominence of deformation on a lesser slip system [100]{021}. The cause of this difference is not obvious but could provide important additional information on the mineral physics involved in the redox reactions and perhaps the shock history of the sample.

[47] For NWA 2737, charge balance requirements ($3Fe^{2+} \rightarrow 2Fe^{3+} + Fe^0$) are fully consistent with the very small amounts of oxidation/reduction needed for the observed presence of Fe^{3+} (<3% total iron) and pervasive $npFe^0$ (~0.1 vol %). It is important to recognize that the small amount of Fe^{3+} that exists in NWA 2737 is completely incapable of producing the dramatic reduction of albedo (transparency of grains) and the pronounced red continuum (increased reflectance toward longer wavelengths) observed throughout the near-infrared for NWA 2737 olivine. Very small amounts of $npFe^0$ in a silicate host produce just those optical properties as long as the size of the metallic particles is <50 nm [*Noble et al.*, 2007].

[48] Thus the well-documented visible, near-infrared, and midinfrared spectral properties of the brown olivine and its related physical and chemical properties indicate that the unusual optical properties (brown color) of NWA 2737 are due to the presence of $npFe^0$ finely dispersed throughout the olivine. Transformation of a normal forsteritic dunite into this brown olivine probably occurred during a massive shock event ~170 Ma ago. Because shocked olivine with

similar optical properties exists in other Martian meteorites (ALH A77005), although less pervasively, the redox conditions on Mars appear to be well suited to this transformation when olivine-bearing lithologies encounter the appropriate level of pressure-temperature conditions during shock [e.g., *Bauer*, 1979].

8. Implications for Remote Sensing

[49] It is not known how commonly the processes leading to the presence of npFe^0-bearing brown olivine occur in the Martian environment. The Martian meteorites are not necessarily representative of the principal geologic terrains on Mars [e.g., *Hamilton et al.*, 2003]. Only one meteorite appears to come from the vast Martian ancient cratered terrain. Nevertheless, it is evident that rocks containing brown olivine were made more than once on Mars (also see discussion and references in work by *Treiman et al.* [2007]). Are these materials relatively common, do they mark important and pervasive products of impact events, or are the meteorite samples we receive on Earth a special but minor subset of Martian geology?

[50] None of the remote sensing techniques currently being applied at Mars can resolve these questions alone. However, when multiple approaches are used in coordination, the added value provides a new dimension to geologic analyses. Three examples are provided below.

[51] 1. If a surface feature exhibits a strong olivine signature at midinfrared wavelengths and equally prominent diagnostic features in the near-infrared, then the feature inherently contains a primary olivine-bearing lithology. It could be volcanic deposits, a deep crustal exposure, or a concentration of unweathered grains plucked out of weaker rocks. Information about the geologic setting and scale of the feature should resolve the options.

[52] 2. If a surface feature exhibits a strong olivine signature at midinfrared wavelengths but a weak or absent signature from olivine in the near-infrared, then the presence of npFe^0-bearing brown olivine as discussed here could be a significant component of, or could dominate, the surface. If the observation is also supported by a relatively low albedo and a red-sloped continuum, then the site is likely to have contained an original olivine-bearing lithology, which has been altered by a significant impact event. This opens additional avenues of investigation. Is the npFe^0-bearing brown olivine associated with basin-scale events? If so, then the distribution of npFe^0-bearing brown olivine provides a particularly good marker for mapping the extent of extreme pressure-temperature conditions associated with such events. On the other hand, is the npFe^0-rich brown olivine associated with impact events of a particular magnitude or random small-scale impact events? If so, craters of a particular size may be particularly useful to delineate the occurrence of ancient olivine-rich lithologies.

[53] 3. If a surface exhibits no olivine signature at midinfrared wavelengths but clear diagnostic features of olivine in the near-infrared, then other physical processes could have been or are still active on the surface. Particle size and texture are known to affect the two measurements differently and provide an additional dimension to the variables studied.

[54] Of course, few measurements do or will lead to such simple or clear-cut observations. Nevertheless, the examples above are end-member cases that will help bound our continued efforts to infer the geological history of Mars through remote compositional analysis of the surface.

9. Issues and Open Questions

[55] There are many possible and very different processes that will produce visually brown olivine. Thus all brown olivines are not all alike, even though they may appear similar to the human eye. We have documented several of the possible causes for colored olivine here, any one of which could occur in different settings. For any given sample of visually brown olivine, several independent approaches should be used in an integrated manner to evaluate the character of the coloration in order to determine its physical causes and the environment under which it formed. Spectroscopy beyond what the human eye detects provides major constraints.

[56] The example shown here with NWA 2737 olivine demonstrates the value that integrated methods (e.g., visible to midinfrared spectroscopy, Mössbauer spectroscopy, detailed petrology, and analytical techniques) provide for understanding the complex character and history of samples. A single technique or observation necessarily relies on experience from previous data; in a new setting this may lead to incorrect assumptions. Initial observations on the color and shock history of Martian brown olivine suggested that shock-induced oxidation is the likely cause of the color, a reasonable hypothesis that turns out nevertheless to be inconsistent with more complete data. Instead, recognition of minor npFe^0 dispersed throughout this Martian visually brown olivine has unexpectedly come to be the best and most complete explanation of the unusual optical properties of this particular type of sample.

[57] But why does npFe^0 develop in some examples of olivine on Mars? The answer is clearly associated with impact processes. No such brown olivine has been observed in lunar samples, however. Why is a modest pO_2 apparently needed? In the case of space-weathering processes on the Moon and asteroids, npFe^0 accumulates on grain rims as deposits from micrometeorite melt vapor or atomic sputtering [*Pieters et al.*, 2000; *Hapke*, 2001]. For the Moon (and asteroids), the process is exterior to rock and soil grains as atoms are mobilized and recondense on the surface. For Mars, there might be a catalyst associated with the more oxidizing environment that makes the process work in the interior of olivine grains at the brief high temperatures and pressures encountered during a major impact event. The presence of apparent shock-induced nanophase metallic iron is now well documented [e.g., *Van de Moortéle et al.*, 2007]. Why do the minor amounts of iron involved appear to have an affinity to be in the Fe^0 state on these very small scales? Although we have documented the case surrounding the occurrence of npFe^0 in olivine on Mars and its prominent effect on observed optical properties, we do not have the answers to these questions and pose them for solution by the community of mineral physicists.

[58] **Acknowledgments.** The RELAB spectroscopy laboratory is a multiuser facility operated under NASA grant NNG06GJ31G. We are grateful to Olywn Menzies and Don Lindsley for providing the synthetic olivines used herein. M.D.L. thanks P. Christensen for the generous use of his emission spectrometer facility at the School of Earth and Space

Exploration, Arizona State University. Treiman's participation is funded in part through the NASA Astrobiology Institute node at Ames Research. Support for this work from the Mars Fundamental Research program and NASA grants NNG04GB53G, NNG04GG12G, NAG5-12687, NAG5-12271, and NAG5-13279 and the ORAU NASA postdoctoral program is gratefully acknowledged. We thank V. Hamilton for a thoughtful review of this manuscript. We are grateful to B. Fectay and C. Bidaut for making NWA 2737 available for study. Lunar and Planetary Institute contribution 1306.

References

Aronson, J. R., A. G. Emslie, and H. G. McLinden (1966), Infrared spectra from particulate surfaces, *Science*, *152*, 345–346, doi:10.1126/science.152.3720.345-a.

Banfield, J. F., M. D. Dyar, and A. V. McGuire (1992), The defect microstructure of oxidized mantle olivine from Dish Hill, California, *Am. Mineral.*, *77*, 977–986.

Bauer, J. F. (1979), Experimental shock metamorphism of mono- and polycrystalline olivine: A comparative study, *Proc. Lunar Planet. Sci. Conf.*, 10th, 2573–2596.

Beck, P., J.-A. Barrat, P. Gillet, I. A. Franchi, R. C. Greenwood, B. Van de Moortele, B. Reynard, M. Bohn, and J. Cotton (2005), The Diderot meteorite: The second chassignite (abstract), *Lunar Planet. Sci.* [CD-ROM], *XXXVI*, abstract 1326.

Beck, P., P. Gillet, J.-A. Barrat, M. Wadhwa, R. C. Greenwood, I. A. Franchi, M. Bohn, J. Cotton, B. Van de Moortele, and B. Reynard (2006), Petrography and geochemistry of the chassignite Northwest Africa 2737 (NWA 2737), *Geochim. Cosmochim. Acta*, *70*, 2127–2139, doi:10.1016/j.gca.2006.01.016.

Berkley, J. L., and K. Keil (1981), Olivine orientation in the ALH A77005 achondrite, *Am. Mineral.*, *66*, 1233–1236.

Bogard, D. D., and D. H. Garrison (2006), Ar-Ar dating of Martian chassignites, NWA 2737 and Chassigny, and nakhlite MIL03346 (abstract), *Lunar Planet. Sci.* [CD-ROM], *XXXVII*, abstract 1108.

Britt, D. T., and C. M. Pieters (1994), Darkening in black and gas-rich ordinary chondrites: The spectral effects of opaque morphology and distribution, *Geochim. Cosmochim. Acta*, *58*, 3905–3919, doi:10.1016/0016-7037(94)90370-0.

Burns, R. G. (1970), Crystal field spectra and evidence for cation ordering in olivine minerals, *Am. Mineral.*, *55*, 1608–1632.

Burns, R. G. (1989), Olivine alteration phases in shergottite ALH A 77005; information from 4.2 degrees K Mössbauer spectra (abstract), *NASA Tech. Memo.*, *4130*, 211–212.

Burns, R. G., and F. E. Huggins (1972), Cation determinative curves for Mg-Fe-Mn olivines from vibrational spectra, *Am. Mineral.*, *57*, 967–985.

Christensen, P. R., J. L. Bandfield, V. E. Hamilton, D. A. Howard, M. D. Lane, J. L. Piatek, S. W. Ruff, and W. L. Stefanov (2000), A thermal emission spectral library of rock-forming minerals, *J. Geophys. Res.*, *105*, 9735–9739, doi:10.1029/1998JE000624.

Conel, J. E. (1969), Infrared emissivities of silicates: Experimental results and a cloudy atmosphere model of spectral emission from condensed particulate mediums, *J. Geophys. Res.*, *74*, 1614–1634, doi:10.1029/JB074i006p01614.

Connolly, H. C., Jr., et al. (2006), The meteoritical bulletin, no. 90, *Meteorit. Planet. Sci.*, *41*, 1383–1418.

Cooper, B. L., J. W. Salisbury, R. M. Killen, and A. E. Potter (2002), Midinfrared spectral features of rocks and their powders, *J. Geophys. Res.*, *107*(E4), 5017, doi:10.1029/2000JE001462.

Cordier, P. (2002), Dislocations and slip systems of mantle mineral, in *Plastic Deformation of Mineral and Rocks*, *Rev. Miner. Geochem.*, vol. 51, edited by S.-I. Jarato and H.-R. Wenk, pp. 137–179, Miner. Soc. Am., Washington, D. C.

Duke, D. A., and J. D. Stephens (1964), Infrared investigation of the olivine group minerals, *Am. Mineral.*, *49*, 1388–1406.

Dunrick, J., A. Legris, and P. Cordier (2005), Influence of crystal chemistry on ideal plastic shear anisotropy in forsterite: First principles calculations, *Am. Mineral.*, *90*, 1072–1077, doi:10.2138/am.2005.1738.

Dyar, M. D. (2003), Ferric iron in SNC meteorites as determined by Mössbauer spectroscopy: Implications for Martian landers and Martian oxygen fugacity, *Meteorit. Planet. Sci.*, *38*, 1733–1752.

Dyar, M. D., A. V. McGuire, and M. D. Harrell (1992), Crystal chemistry of iron in contrasting styles of metasomatism in the upper mantle, *Geochim. Cosmochim. Acta*, *56*, 2579–2586, doi:10.1016/0016-7037(92)90212-2.

Fabian, D., T. Henning, C. Jager, H. Mutschke, J. Dorschner, and O. Wehrhan (2001), Steps toward interstellar silicate mineralogy: VI. Dependence of crystalline olivine IR spectra on iron content and particle shape, *Astron. Astrophys.*, *378*, 228–238, doi:10.1051/0004-6361:20011196.

Goodrich, C. A. (2003), Petrogenesis of olivine-phyric shergottites Sayh al Uhaymir 005 and Elephant Moraine 79001 lithology A, *Geochim. Cosmochim. Acta*, *67*, 3735–3772, doi:10.1016/S0016-7037(03)00171-6.

Hamilton, V. E., P. R. Christensen, H. Y. McSween Jr., and J. L. Bandfield (2003), Searching for the source regions of Martian meteorites using MGS TES: Integrating Martian meteorites into the global distribution of igneous materials on Mars, *Meteorit. Planet. Sci.*, *38*, 871–885.

Hapke, B. (2001), Space weathering from Mercury to the asteroid belt, *J. Geophys. Res.*, *106*, 10,039–10,073, doi:10.1029/2000JE001338.

Hofmeister, A. M. (1997), Infrared reflectance spectra of fayalite, and absorption data from assorted olivines, including pressure and isotope effects, *Phys. Chem. Miner.*, *24*, 535–546, doi:10.1007/s002690050069.

Hunt, G. R., and R. K. Vincent (1968), The behavior of spectral features in the infrared emission from particulate surfaces of various grain sizes, *J. Geophys. Res.*, *73*, 6039–6046, doi:10.1029/JB073i018p06039.

Ikeda, Y. (1994), Petrography and petrology of the ALH-77005 shergottite, *Proc. NIPR Symp. Antarct. Meteorites*, *7*, 9–29.

Jeanloz, R. (1980), Infrared spectra of olivine polymorphs: α, β phase and spinel, *Phys. Chem. Miner.*, *5*, 327–341, doi:10.1007/BF00307542.

King, T. V. V., and W. I. Ridley (1987), Relation of the spectroscopic reflectance of olivine to mineral chemistry and some remote sensing implications, *J. Geophys. Res.*, *92*, 11,457–11,469, doi:10.1029/JB092iB11p11457.

Lane, M. D. (1999), Midinfrared optical constants of calcite and their relationship to particle size effects in thermal emission spectra of granular calcite, *J. Geophys. Res.*, *104*, 14,099–14,108, doi:10.1029/1999JE900025.

Lane, M. D., and M. D. Dyar (2007), Thermal emission spectroscopy of synthetic olivines: Fayalite to forsterite (abstract), *Meteorit. Planet. Sci.*, *42*, suppl., abstract 5136.

McFadden, L. A., and T. P. Cline (2005), Spectral reflectance of Martian meteorites: Spectral signatures as a template for locating source region on Mars, *Meteorit. Planet. Sci.*, *41*, 151–172.

McGuire, A. V., M. D. Dyar, and J. E. Nielson (1991), Metasomatic oxidation of upper mantle peridotite, *Contrib. Mineral. Petrol.*, *109*, 252–264, doi:10.1007/BF00306483.

McSween, H. Y., Jr. (2002), The rocks of Mars, from far and near, *Meteorit. Planet. Sci.*, *37*, 7–25.

McSween, H. Y., Jr., L. A. Taylor, and E. M. Stolper (1979), Allan Hills 77005: A new meteorite type found in Antarctica, *Science*, *204*, 1201–1203, doi:10.1126/science.204.4398.1201.

Menzies, O. N., P. A. Bland, and F. J. Berry (2001), An ^{57}Fe Mössbauer study of the olivine solid solution series: Implications for meteorite classification and deconvolution of unequilibrated chondrite spectra, *Lunar Planet. Sci.* [CD-ROM], XXXII, abstract 1622.

Mikouchi, T. (2005), Comparative mineralogy of Chassigny and NWA 2737: Implications for the formation of chassignite igneous body(s) (abstract), *Meteorit. Planet. Sci.*, *40*, abstract 5240.

Misawa, K., C.-Y. Shih, Y. Reese, L. E. Nyquist, and J.-A. Barrat (2005), Rb-Sr and Sm-Nd isotopic systematics of NWA 2737 chassignite (abstract), *Meteorit. Planet. Sci.*, *40*, abstract 5200.

Mustard, J. F., and J. E. Hays (1997), Effects of hyperfine particles on reflectance spectra from 0.3 to 25 μm, *Icarus*, *125*, 145–163, doi:10.1006/icar.1996.5583.

Noble, S. K., C. M. Pieters, and L. P. Keller (2007), An experimental approach to understanding the optical effects of space weathering, *Icarus*, *192*, 629–642, doi:10.1016/j.icarus.2007.07.021.

Ostertag, R., G. Amthauer, H. Rager, and H. Y. McSween Jr. (1984), Fe^{3+} in shocked olivine crystals of the ALHA 77005 meteorite, *Earth Planet. Sci. Lett.*, *67*, 162–166, doi:10.1016/0012-821X(84)90111-0.

Pieters, C. M., and T. Hiroi (2004), RELAB (Reflectance Experiment Laboratory): A NASA multiuser spectroscopy facility (abstract), *Lunar Planet. Sci.* [CD-ROM], XXXV, abstract 1720.

Pieters, C. M., L. A. Taylor, S. K. Noble, L. P. Keller, B. Hapke, R. V. Morris, C. C. Allen, D. A. McKay, and S. Wentworth (2000), Space weathering on airless bodies: Resolving a mystery with lunar samples, *Meteorit. Planet. Sci.*, *35*, 1101–1107.

Redfern, S. A. T., G. Artioli, R. Rinaldi, C. M. B. Henderson, K. S. Knight, and B. J. Wood (2000), Octahedral cation ordering in olivine at high temperature. II: An in situ neutron powder diffraction study on synthetic MgFeSiO4 (Fa50), *Phys. Chem. Miner.*, *27*, 630–637, doi:10.1007/s002690000109.

Reynard, B., B. van Moortele, P. Beck, and P. Gillet (2006), Shock-induced transformations in olivine of the chassignite NWA 2737, *Lunar Planet. Sci.* [CD-ROM], *XXXVII*, abstract 1837.

Ruff, S. W., P. R. Christensen, P. W. Barbera, and D. L. Anderson (1997), Quantitative thermal emission spectroscopy of minerals: A laboratory technique for measurement and calibration, *J. Geophys. Res.*, *102*, 14,899–14,913, doi:10.1029/97JB00593.

Salisbury, J. W. (1993), Mid-infrared spectroscopy: Laboratory data, in *Remote Geochemical Analysis: Elemental and Mineralogical Composition*, edited by C. M. Pieters and P. A. Englert, pp. 79–98, Cambridge Univ. Press, Cambridge, U. K.

Salisbury, J. W., and J. W. Eastes (1985), The effect of particle size and porosity on spectral contrast in the mid-infrared, *Icarus*, *64*, 586–588, doi:10.1016/0019-1035(85)90078-8.

Sunshine, J. M., and C. M. Pieters (1998), Determining the composition of olivine from reflectance spectroscopy, *J. Geophys. Res.*, *103*, 13,675–13,688, doi:10.1029/98JE01217.

Tarte, P. (1963), Infrared study of orthosilicates and orthogermanates. II. Olivine and monticellite structures, *Spectrochim. Acta, Part A*, *19*, 25–47.

Treiman, A. H., J. D. Gleason, and D. D. Bogard (2000), The SNC meteorites are from Mars, *Planet. Space Sci.*, *48*, 1213–1230, doi:10.1016/S0032-0633(00)00105-7.

Treiman, A. H., M. D. Dyar, M. McCanta, C. M. Pieters, T. Hiroi, M. D. Lane, and J. Bishop (2007), Martian dunite NWA 2737: Petrographic constraints on geologic history, shock events, and olivine color, *J. Geophys. Res.*, *112*, E04002, doi:10.1029/2006JE002777.

Van de Moortéle, B., B. Reynard, P. Rochette, M. Jackson, P. Beck, P. Gillet, P. F. McMillan, and C. A. McCammon (2007), Shock-induced metallic iron nanoparticles in olivine-rich Martian meteorites, *Earth Planet. Sci. Lett.*, *262*, 37–49, doi:10.1016/j.epsl.2007.07.002.

Wivel, C., and S. Mørup (1981), Improved computational procedure for evaluation of overlapping hyperfine parameter distributions in Mössbauer spectra, *J. Phys. E Sci. Instrum.*, *14*, 605–610, doi:10.1088/0022-3735/14/5/018.

J. L. Bishop, NASA-Ames Research Center, Mail Stop 239-4, Mountain View, CA 94043, USA.

M. D. Dyar, Department of Astronomy, Mount Holyoke College, South Hadley, MA 01075, USA.

T. Hiroi, R. L. Klima, and C. M. Pieters, Department of Geological Sciences, Brown University, 324 Brook Street, Providence, RI 02912, USA. (carle_pieters@brown.edu)

M. D. Lane, Planetary Science Institute, 1700 E. Ft. Lowell, Suite 106, Tucson, AZ 85719, USA.

S. K. Noble, Astromaterials Research and Exploration Science Division, Johnson Space Center, Houston, TX 77058, USA.

J. M. Sunshine, Department of Astronomy, University of Maryland, College Park, MD 20742, USA.

A. H. Treiman, Lunar and Planetary Institute, 3600 Bay Area Boulevard, Houston, TX 77058, USA.